Received: 19 November 2018 | Revised: 26 April 2019 | Accepted: 5 July 2019

DOI: 10.4218/etrij.2018-0639

ORIGINAL ARTICLE

ETRI Journal WILEY

Gait event detection algorithm based on smart insoles

JeongKyun Kim[1,2] | **Myung-Nam Bae**[2] | **Kang Bok Lee**[2] | **Sang Gi Hong**[1,2]

[1]School of Computer Software, ICT, University of Science and Technology, Daejeon, Rep. of Korea

[2]Intelligent Convergence Research Laboratory, Electronics and Telecommunications Research Institute, Daejeon, Rep. of Korea

Correspondence
Sang Gi Hong, Intelligent Convergence Research Laboratory, Electronics and Telecommunications Research Institute, Daejeon, Rep. of Korea.
Email: sghong@etri.re.kr

Funding information
This research was supported by 'The Cross-Ministry Giga KOREA Project' grant funded by the Korea government (MSIT) (Development and Validation of 5G Based Disaster Safety Services, GK18P0900) and was supported by a grant (19DRMS-B146826-02) from Development of Customized Contents Provision Technology for Realistic Disaster Management Based on Spatial Information Program funded by Ministry of the Interior and Safety of Korean government.

Gait analysis is an effective clinical tool across a wide range of applications. Recently, inertial measurement units have been extensively utilized for gait analysis. Effective gait analyses require good estimates of heel-strike and toe-off events. Previous studies have focused on the effective device position and type of triaxis direction to detect gait events. This study proposes an effective heel-strike and toe-off detection algorithm using a smart insole with inertial measurement units. This method detects heel-strike and toe-off events through a time-frequency analysis by limiting the range. To assess its performance, gait data for seven healthy male subjects during walking and running were acquired. The proposed heel-strike and toe-off detection algorithm yielded the largest error of 0.03 seconds for running toe-off events, and an average of 0–0.01 seconds for other gait tests. Novel gait analyses could be conducted without suffering from space limitations because gait parameters such as the cadence, stance phase time, swing phase time, single-support time, and double-support time can all be estimated using the proposed heel-strike and toe-off detection algorithm.

KEYWORDS
gait analysis, heel-strike detection, smart insole, time-frequency analysis, toe-off detection

1 | INTRODUCTION

Many people suffer from spine and nerve diseases, some of which can be evaluated through physical activities. Walking is one of the most common physical activities; therefore, there has been increasing clinical and research interest in gait monitoring. Gait analysis systems are employed both to evaluate patient health conditions and study the gait [1–4]. Gait analysis is an effective clinical tool for a wide range of applications, such as assessing neurological diseases [5], the risk of falls [6], orthopedic disabilities, and rehabilitation progress [7,8]. Conventional clinical gait analysis methods are based on motion-capture systems [9,10] and force plates [11], which offer a high accuracy in measuring gait events. Unfortunately, these approaches only provide information on a couple of steps, and they are highly expensive and space-consuming. Inertial measurement units (IMUs) have recently been utilized in many walking studies because they are not time- or space-consuming, are inexpensive, and can provide kinematic information [12]. IMUs include both accelerometers and gyroscopes, and can therefore be used to measure triaxial accelerations and rotations during gait events. The rich and continuous gait data acquired from IMUs provide a variety of information for clinical research, and demonstrate considerable potential for remote diagnosis.

Several spatiotemporal parameters, such as stride time, stance phase time, swing phase time, stride frequency, and stride length, must be determined for gait analysis [13–15]. The gait cycle begins when the heel of one foot touches the

ground during the stepping process, and ends with the next step of the same foot. Each cycle includes both a stance phase and swing phase. The stance phase, during which the foot touches the ground, goes from heel-strike (HS: when the heel touches the ground) to toe-off (TO: when the toe lifts off the ground). The swing phase, during which the foot moves separately from the ground, goes from TO to the next HS of the same foot. On average, the stance and swing phases account for 60% and 40% of the gait cycle duration, respectively [16].

When both feet are in contact with the ground during the gait cycle, this is called the double-support phase. When only the right or left foot is in contact with the ground, this is called the single-support phase. As the walking speed increases, the swing phase becomes proportionally longer, and both the single and double stance phases become shorter. A loss of the double stance indicates a transition from walking to running: a condition in which completely airborne phases occur with the body not touching the ground at all [17]. These concepts are illustrated in Figure 1.

To accurately identify and characterize these different phases of the gait cycle, gait events such as HS and TO must be detected. Recently, various methods have been proposed using IMUs attached to the foot, shank, or waist. The foot is likely to be a suitable location for detecting gait events, because it produces a clear distinction between the stance and swing phases and imposes very little restriction on muscle contractions and joint movements during walking [18–20].

Several studies have reported methods to detect gait events using accelerometers or gyroscopes attached to various locations, such as the shank [21], neck [22], waist [23], and foot [14,18,19]. It is easier to detect gait events from the foot, because it is closer to the ground. The simplest gait event detection methods are peak identification and thresholding. More advanced methods involve signal processing and machine learning techniques such as neural networks [24], hidden Markov models [25], and Gaussian mixture models [26]. Machine learning requires data for learning, and data collection is difficult because there are many differences depending on a person's gait.

For example, using the foot to detect the gait, Misu and others [18] employed a method to determine gait events by detecting HS using acceleration data and TO using angular velocity data.

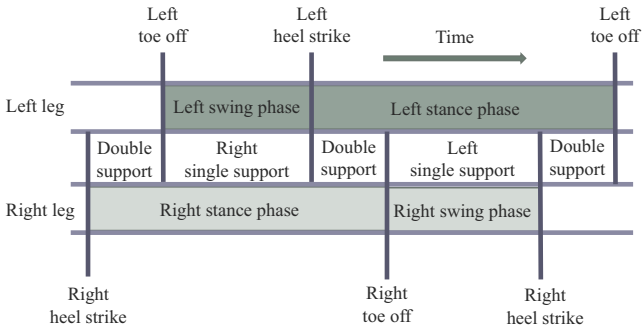

FIGURE 1 Gait cycle

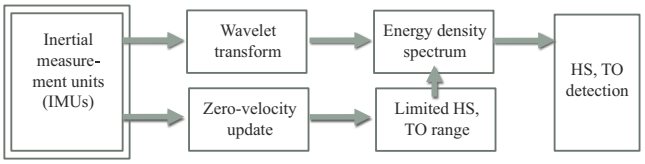

FIGURE 2 Overview of the proposed method

Angular velocity data have the significant advantage that they are not affected by gravity. However, gyroscopes consume a lot of power, and therefore, accelerometers are also increasingly being utilized. Mo and others [27] identified HS as the instant of peak resultant acceleration using a threshold, and identified TO as the moment at which the acceleration exceeds a threshold of 2g (g = gravitational acceleration). Khandelwal and others [19] proposed a time-frequency analysis of acceleration signals to detect HS and TO. Although these methods yield good performances, they are not sufficient to detect TO when IMUs are attached to the insole. Therefore, we propose an effective method to detect gait events using a smart insole with IMUs. This method detects HS and TO through a time-frequency analysis by limiting the range. Figure 2 presents an overview of this method.

This paper is organized as follows: Section 2 presents the proposed HS and TO detection methods. The experiment and results are described in Section 3, and Section 4 discusses the results. Finally, conclusions are presented in Section 5.

2 | MATERIALS AND METHODS

2.1 | Gait data

We acquired gait data from seven healthy subjects (males) with average an age, height, and weight of 29 years, 175 cm, and 74 kg, respectively. The gait data consists of inertial data acquired from the left and right insoles and pressure data acquired from the insoles.

Pressure sensors were placed at the outer toe, inner toe, inner heel, outer heel, and midfoot. These were used as comparison standards for gait events. Gait data were acquired using an MPU 9250 motion processing unit (InvenSense Inc.) with Three axes accelerometers, gyroscopes, and compasses. The accelerometers have a programmable range of 2g, 4g, 8g, and 16g; and the gyroscopes can operate with ranges of 125 °/s, 250 °/s, 500 °/s, and 1000 °/s. In the experiments, the accelerometer range was set to 8g, the gyroscope range to 1000 °/s, and the sampling frequency to 100 Hz, as shown in Figure 3.

2.2 | Zero-velocity update

The zero-velocity update (ZUPT) method is widely employed to estimate the stance phase in pedestrian dead-reckoning (PDR), a type of personal navigation system based on inertial sensors that does not require any infrastructure.

FIGURE 3 Smart insoles

Skog [28] proposed a ZUPT method called the general likelihood ratio test (GLRT), which employs a probability to determine whether the average magnitudes of the acceleration and angular velocity are below a certain threshold, as shown in (1). In this equation, $a_n \in R^3$ and $\omega_n \in R^3$ denote the triaxial acceleration and angular velocity at the nth sample, respectively; σ_a and σ_ω denote the accelerometer and gyroscope noise variances; respectively; γ denotes the threshold; and W is the window size [29].

$$\frac{1}{W}\sum_{k=n}^{n+W-1}\frac{1}{\sigma_a^2}\left\|a_k - g\frac{\overline{a}_n}{|\overline{a}_n|}\right\|^2 + \frac{1}{\sigma_\omega^2}\|\omega_k\|^2 < \gamma, \quad (1)$$

$$\overline{a}_n = \frac{1}{W}\sum_{k=n}^{n+W-1} a_k. \quad (2)$$

Figure 4 shows an example of the results obtained using this method. Here, Acc denotes a composite acceleration signal and ZUPT is the estimated zero-velocity duration.

The GLRT method yields a good performance for PDR. It is not significantly affected by a small number of false detections, but it can detect false gait events. ZUPT is determined by the threshold γ, which varies according to the gait velocity, because the baseline increases, as shown in Figure 5A. In this study, we developed an adaptive ZUPT approach consisting of three stages. First, the gait signal

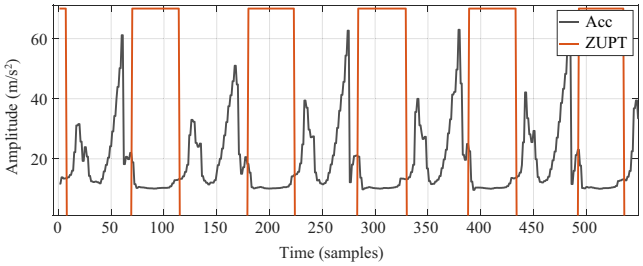

FIGURE 4 Zero-velocity update

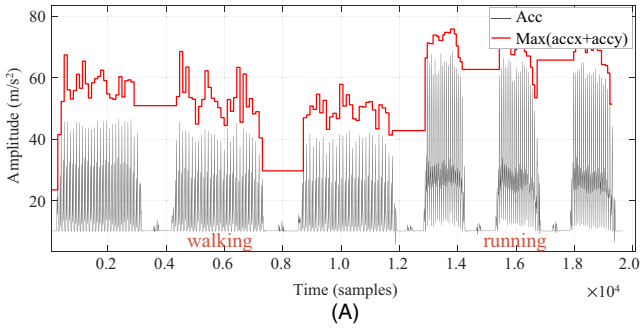

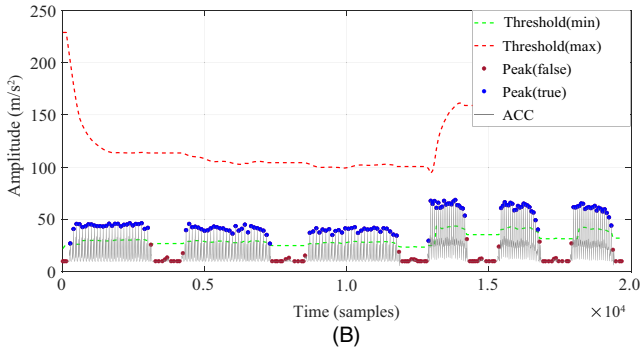

FIGURE 5 (A) The baseline, which increases with the gait velocity, and (B) peak detection using an adaptive threshold to determine the step

periodically exhibits a high peak during each step. This peak is determined by the adaptive minimum-maximum threshold. A new peak represents a local maximum when observing that the signal changes direction within a predefined time interval. The new peak is distinguished by a false or true peak, and the procedure is defined as follows and illustrated in Figure 5B:

$$\begin{aligned}
&\text{if } (\text{Threshold}_{\text{min}} < \text{Peak}_{\text{new}})\{\text{Peak}_{\text{signal},n} = \text{Peak}_{\text{new}}\},\\
&\text{else } \{\text{Peak}_{\text{noise},n} = \text{Peak}_{\text{new}}\};\\
&\text{PB}_{\text{noise}} = \{\text{Peak}_{\text{noise},n}, \text{Peak}_{\text{noise},n-1}, \text{Peak}_{\text{noise},n-2},\\
&\quad \text{Peak}_{\text{noise},n-3}\};\\
&\text{PB}_{\text{signal}} = \{\text{Peak}_{\text{signal},n}, \text{Peak}_{\text{signal},n-1}, \text{Peak}_{\text{signal},n-2},\\
&\quad \text{Peak}_{\text{signal},n-3}\};\\
&\text{Threshold}_{\text{min}} = \text{PB}_{\text{noise,median}} + (\text{PB}_{\text{signal,median}} -\\
&\quad \text{PB}_{\text{noise,median}}) \times 0.6;\\
&\text{Threshold}_{\text{max}} = 0.8 \times \text{Threshold}_{\text{max}} + 0.1 \times \text{PB}_{\text{signal,max}}\\
&\quad + 0.4 \times \text{PB}_{\text{signal,median}};\\
&\text{if } (\text{Threshold}_{\text{min}} < \text{Peak}_{\text{new}} < \text{Threshold}_{\text{max}}) \{\text{Peak}_{\text{true}} =\\
&\quad \text{Peak}_{\text{new}}\},\\
&\text{else } \{\text{Peak}_{\text{false}} = \text{Peak}_{\text{new}}\};
\end{aligned}$$

Second, the interval from the current $\text{Peak}_{\text{true}}$ to the next $\text{Peak}_{\text{true}}$ is one step, and the ZUPT threshold is determined based on the maximum speed of one step. Third, if there are two ZUPT intervals within one step, then the longest interval is the ZUPT interval.

2.3 | Time-frequency analysis

The gait cycle is periodically repeated in four steps: stance (ST), TO, swing (SW), and HS. The HS step precedes ST, and the TO step follows ST [30]. The HS detection range is therefore selected as the one-third section from the end point of the previous zero-velocity region to the starting point of the present zero-velocity region, and the TO range is selected as the one-third section from the end point of the present zero-velocity region to the starting point of the next zero-velocity region.

When HS and TO occur, physical events occur between the foot and ground, and these are detected using a time-frequency analysis. The time-frequency characteristics of gait cycles have been utilized in previous studies [19,31]. The present study employs Acc to detect a gait event. However, Acc contains a lot of additional information, such as the movement signal and noise, especially during running. Therefore, it is better to detect HS using the x-axis and TO using the z-axis rather than by using Acc, because the x-axis acceleration increases in the swing phase and decreases rapidly in HS. Furthermore, the z-axis acceleration increases in TO, as shown in Figure 6.

Haar proposed the wavelet transform in the early 1900s [32]. The wavelet transform produces a time-frequency decomposition of a signal, in which the individual signal components are separated. This approach enables peak detection to be performed more effectively than with the short-time Fourier transform.

In the wavelet transform, mother wavelets are based on small waves with varying frequencies and limited durations. In this study, we employ the Morlet wavelet, which is widely utilized for analyzing biological signals for gait event detection. The Morlet wavelet is defined as in (3). Here, ω_0 is the frequency and η is the time parameter [33–35].

$$\psi_0(\eta) = -\pi^{-\frac{1}{4}} e^{i\omega_0\eta} e^{-\frac{\eta^2}{2}}, \tag{3}$$

$$W_n(s) = \sum_{\acute{n}=0}^{N-1} x_{\acute{n}} \psi^* \left[\frac{(\acute{n}-n)\,\delta_t}{s} \right]. \tag{4}$$

The continuous wavelet transform (CWT) is defined as a function of both the mother wavelet $\psi_0(\eta)$ and signal x_n, as in (4). In this equation, * denotes the complex conjugate, s is the wavelet scaling factor, δ_t is the (uniform) time spacing, and n is the localized time index.

Figure 7A depicts the results of applying the continuous wavelet transform to the composite acceleration signal with a varying scaling factor to detect gait events. The smaller the scale, the higher the frequency. Therefore, the representation at larger scales corresponds to lower-frequency signal components. This figure confirms that HS and TO occur regularly in the high-frequency range. The energy density spectrum E_{ds} was obtained from the coefficients of the CWT of the composite acceleration signal, as shown in (5), where s is the scale [34,35].

$$E_{ds} = \sum_{n=0}^{N-1} |W_n(s)|^2, \tag{5}$$

$$s \in [1, s_{max}]. \tag{6}$$

In the energy density spectrum obtained from the squares of the x-axis and z-axis acceleration signals, the largest peaks in the 20–40 scale range are denoted by S_{TO} and S_{HS},

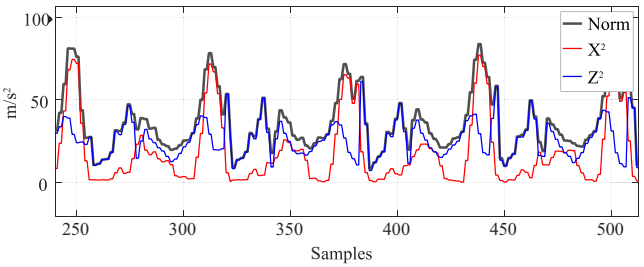

FIGURE 6 Squares of x-axis and z-axis acceleration signals

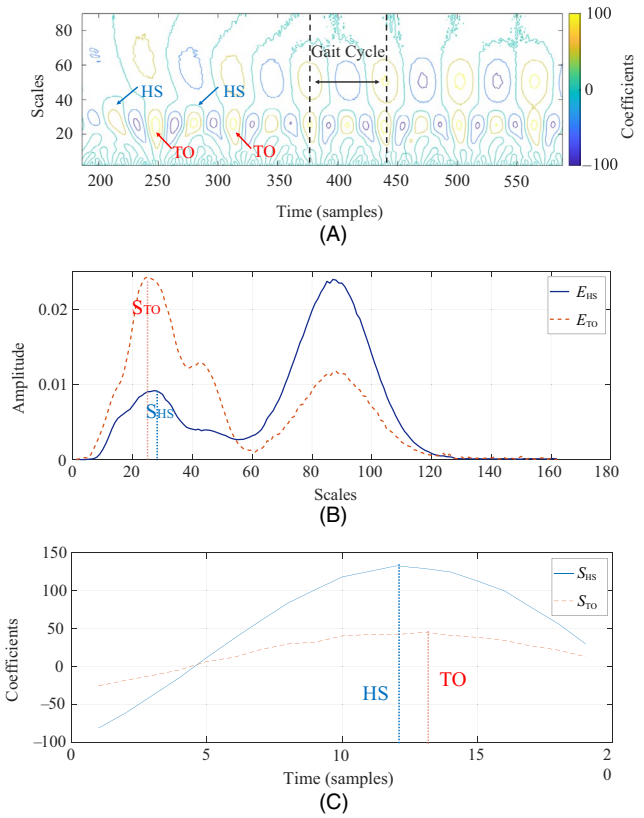

FIGURE 7 (A) Results of applying the continuous wavelet transform to the composite acceleration signal. (B) The energy density spectra obtained from the CWT coefficients of the squares of the x-axis and z-axis acceleration signals. (C) The CWT coefficients of the scales in the limited HS and TO ranges

TABLE 1 Walking HS and TO detection results. Units: samples (standard deviation)

Walking	Left HS MAE (STD)	Left TO MAE (STD)	Right HS MAE (STD)	Right TO MAE (STD)
Mo [27]	1.96 (2.51)	5.65 (2.21)	1.61 (1.37)	5.78 (1.18)
Misu [18]	1.96 (2.51)	3.45 (6.29)	1.61 (1.37)	3.48 (4.78)
Siddhartha [19]	3.09 (2.39)	6.39 (3.01)	4.46 (3.63)	10.47 (3.20)
P.M	1.08 (0.74)	0.88 (0.70)	0.99 (0.82)	1.97 (0.93)

TABLE 2 Running HS and TO detection results. Units: samples (standard deviation)

Running	Left HS MAE (STD)	Left TO MAE (STD)	Right HS MAE (STD)	Right TO MAE (STD)
Mo [27]	3.09 (1.01)	8.97 (3.50)	2.95 (1.11)	10.11 (4.11)
Misu [18]	3.09 (1.01)	5.47 (1.65)	2.95 (1.11)	7.59 (4.33)
Siddhartha [19]	2.44 (1.18)	3.79 (1.09)	2.63 (1.33)	5.21 (3.44)
P.M	0.87 (1.06)	2.53 (1.97)	0.67 (0.52)	2.76 (1.44)

TABLE 3 Walking test result on the treadmill. Units: percent (standard deviation)

	Right (%)	Left (%)
Cadence: 70 step/min (3 km)		
Stance	66 (0.01)	66 (0.01)
Single support time	34 (0.02)	34 (0.02)
Double support time	31 (0.04)	N/A
Cadence: 79 step/min (4 km)		
Stance	58 (0.01)	58 (0.01)
Single support time	43 (0.02)	43 (0.02)
Double support time	15 (0.08)	N/A
Cadence: 90 step/min (5 km)		
Stance	52 (0.01)	52 (0.01)
Single support time	46 (0.02)	46 (0.02)
Double support time	6 (0.03)	N/A

respectively, as shown in Figure 7B. In this study, the maximum values of the CWT coefficients of S_{TO} and S_{HS} within the HS and TO ranges are selected as the HS and TO points, as shown in Figure 7C.

3 | EXPERIMENT AND RESULTS

To analyze the results of the proposed HS and TO detection algorithms, we utilized data measured from triaxial inertial sensors attached to the insole. Three walking and running datasets were constructed to evaluate the algorithm. These data were collected from seven male subjects aged 27–33 years. The subjects were briefed on the purpose of the study and the method before their consent was obtained. Table 1 presents the obtained mean and standard deviation of the time differences (in the number of samples) between the gait events (HS and TO) obtained by the inertial sensors, and the gait events (HS and TO) obtained by the pressure sensors on the toe and heel.

The proposed HS and TO detection algorithms were implemented in MATLAB, and yielded the largest error of three samples (0.03 seconds) for the running TO and an average of 0–1 samples (0–0.01 seconds) for the other gait tests (see Tables 1 and 2). The error in the running TO case is relatively large, because the gait speed is relatively high. This may lead to inaccuracies in the detection of gait signal events.

4 | DISCUSSION

Gait parameters, such as the cadence, stance time, single-support time, and double-support time, were calculated using the detected HS and TO events. The validity of the proposed gait analysis algorithm is verified by comparing the parameters for 3-, 4-, and 5-km/h walks on the treadmill.

As the treadmill speed increases, the cadence increases from 70 steps/min (3 km/h) to 90 steps/min (5 km/h), the stance phase time decreases, the single-support time increases, and the double-support time decreases, as shown in Table 3. This result is similar to those of previous studies, in that when the gait speed increases the stance phase time decreases, the swing phase time increases, and the double-support time decreases. In fact, the double-support time disappears during running.

To analyze the three-dimensional (3D) motion pattern of the continuous walking cycle, the measured gait acceleration and angular velocity signals were separated by the HS points of each individual walking step. Figure 8 depicts the resulting 3D kinematic pattern, which can be used to analyze the gait.

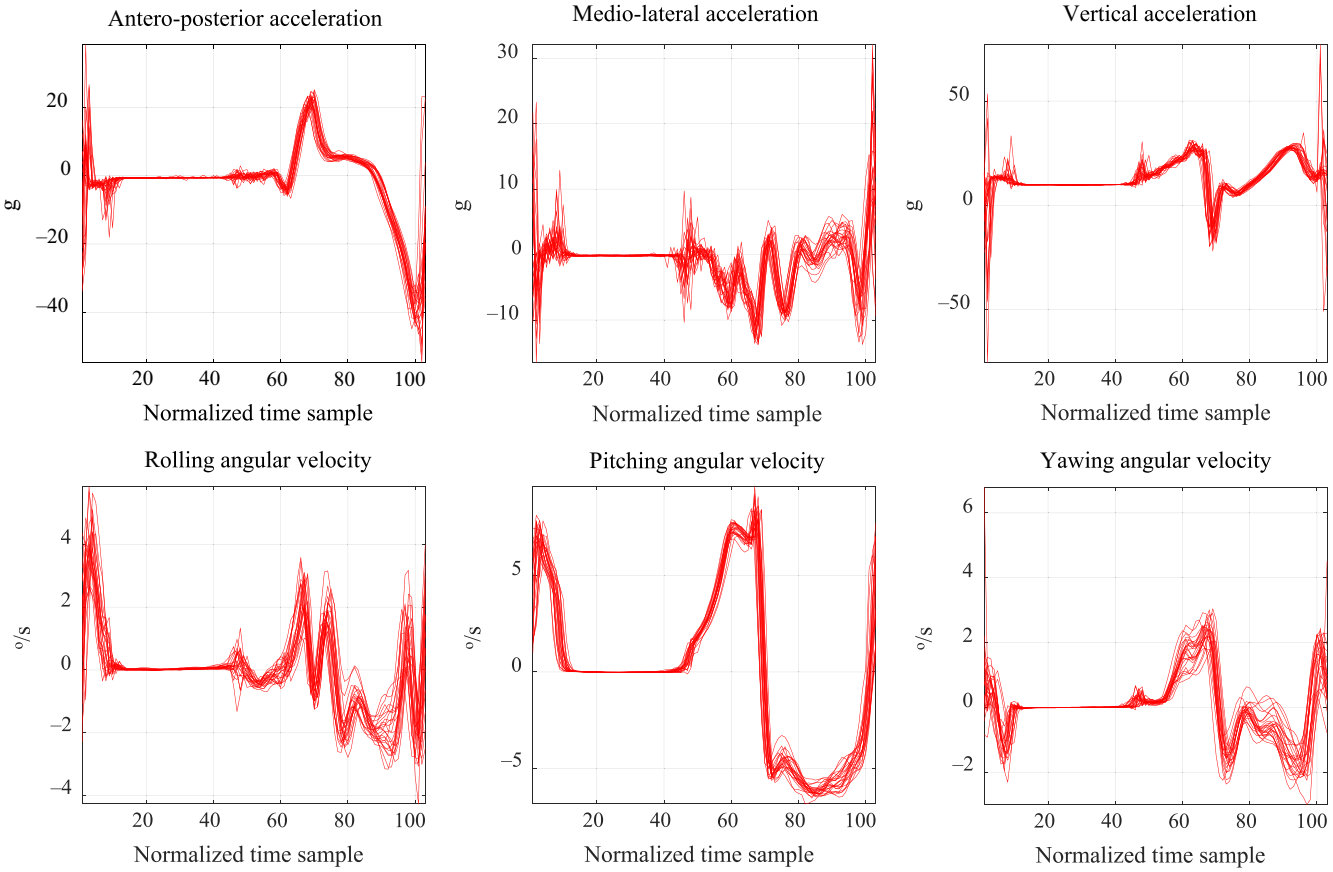

FIGURE 8 3D kinematic pattern

5 | CONCLUSIONS

Inertial sensors are becoming increasingly popular, owing to interest in the development and health benefits of wearable devices. Thus far, gait analysis methods have only been employed in specific locations, such as hospitals and laboratories, and have only been applied to patients. However, as healthcare becomes more important owing to an aging population, westernized eating habits, and youth health problems, simple measurements of users' gaits in everyday life are becoming increasingly necessary. Therefore, in this study, we developed a method to analyze the gait during common daily life activities using an inertial sensor.

The gait parameter detection algorithm is based on the triaxial acceleration and gyroscopic signals measured using an inertial sensor during walking. The obtained average error was below 0.02 seconds in walking and running.

The cadence, stance time, single-support time, and double-support time can all be estimated using the proposed gait parameter detection algorithm. Furthermore, three linear motions (anterior-posterior, medial-lateral, and superior-inferior) and three rotational motions (inversion-eversion, dorsi-plantar, and adduction-abduction) can be obtained.

Therefore, the proposed method can be utilized to manage and correct gait during everyday life activities, not just in hospital environments. Furthermore, novel gait analysis studies could be conducted without suffering from space limitations, and so this approach can be utilized for exercise monitoring and fall detection by analyzing daily-life behavior. However, given that additional variables need to be considered in real-world experiments, further studies must be conducted to verify and improve the algorithms and make them robust in broader and more general types of situations.

ORCID

JeongKyun Kim https://orcid.org/0000-0003-1822-1752
Sang Gi Hong https://orcid.org/0000-0001-8135-3286

REFERENCES

1. K. Ziegler-Graham et al., *Estimating the prevalence of limb loss in the United States: 2005 to 2050*, Archives Phys. Medicine Rehabilitation **89** (2008), no. 3, 422–429.
2. M. Bellmann, T. Schmalz, and S. Blumentritt, *Comparative biomechanical analysis of current microprocessor-controlled prosthetic knee joints*, Archives Phys. Medicine Rehabilitation **91** (2010), no. 4, 644–652.

3. M. Hanlon and R. Anderson, *Real-time gait event detection using wearable sensors*, Gait Posture **30** (2009), no. 4, 523–527.
4. J. J. Kavanagh and H. B. Menz, *Accelerometry: a technique for quantifying movement patterns during walking*, Gait Posture **28** (2008), no. 1, 1–15.
5. A. K. Rao, L. Quinn, and K. S. Marder, *Reliability of spatiotemporal gait outcome measures in Huntington's disease*, Mov Disord **20** (2005), no. 8, 1033–1037.
6. J. M. Hausdorff, D. A. Rios, and H. K. Edelberg, *Gait variability and fall risk in community-living older adults: a 1-year prospective study*, Archives Phys. Medicine Rehabilitation **82** (2001), no. 8, 1050–1056.
7. J. A. DeLisa (Ed.), *Gait analysis in the science of rehabilitation*, vol **2**, Diane Publishing, Washington, D.C., 1998.
8. O. Bello et al., *Spatiotemporal parameters of gait during treadmill and overground walking in Parkinson's disease*, J. Parkinson's Disease **4** (2014), no. 1, 33–36.
9. A. Pfister et al., *Comparative abilities of Microsoft Kinect and Vicon 3D motion capture for gait analysis*, J. Medical Eng. Technol. **38** (2014), no. 4, 274–280.
10. T. B. Moeslund, A. Hilton, and V. Krüger, *A survey of advances in vision-based human motion capture and analysis*, Comput. Vision Image Understanding **104** (2006), 90–126.
11. B. D. Hendershot, C. E. Mahon, and L. A. Pruziner, *A comparison of kinematic-based gait event detection methods in a self-paced treadmill application*, J. Biomechan. **49** (2016), no. 16, 4146–4149.
12. P. B. Shull et al., *Quantified self and human movement: a review on the clinical impact of wearable sensing and feedback for gait analysis and intervention*, Gait Posture **40** (2014), no. 1, 11–19.
13. P. Esser et al., *Assessment of spatio-temporal gait parameters using inertial measurement units in neurological populations*, Gait Posture **34** (2011), no. 4, 558–560.
14. F. Dadashi et al., *Gait and foot clearance parameters obtained using shoe-worn inertial sensors in a large-population sample of older adults*, Sensors **14** (2013), no. 1, 443–457.
15. Y. K. Kim et al., *Effects of walking speed and age on the directional stride regularity and gait variability in treadmill walking*, J. Mechan. Sci. Technol. **30** (2016), no. 6, 2899–2906.
16. M. P. Murray, *Gait as a total pattern of movement: Including a bibliography on gait*, Am. J. Phys. Medicine Rehabilitation **46** (1967), no. 1, 290–333.
17. M. W. Whittle, *Clinical gait analysis: A review*. Human Movement Science **15**, 1996, no. 3, 369–387.
18. S. Misu et al., *Development and validity of methods for the estimation of temporal gait parameters from heel-attached inertial sensors in younger and older adults*, Gait Posture **57** (2017), 295–298.
19. S. Khandelwal and N. Wickström, *Gait event detection in real-world environment for long-term applications: Incorporating domain knowledge into time-frequency analysis*, IEEE Trans. Neural Syst. Rehabilitation Eng. **24** (2016), no. 12, 1363–1372.
20. W. Zijlstra and A. L. Hof, *Assessment of spatio-temporal gait parameters from trunk accelerations during human walking*, Gait Posture **18** (2003), no. 2, 1–10.
21. M. Djuric, *Automatic recognition of gait phases from accelerations of leg segments*, In Proc. Symp. Neural Netw. Applicat. Electr. Eng., Belgrade, Serbia, Sept. 2008, pp. 121–124.
22. J. M. Jasiewicz et al., *Wireless orientation sensors: their suitability to measure head movement for neck pain assessment*, Manual Therapy **12** (2007), no. 4, 380–385.
23. C. Soaz and K. Diepold, *Step detection and parameterization for gait assessment using a single waist-worn accelerometer*, IEEE Trans. Biomedical Eng. **63** (2016), no. 5, 933–942.
24. E. Tileylioğlu and A. Yilmaz. *Application of neural based estimation algorithm for gait phases of above knee prosthesis*, In Proc. Annu. Int. Conf. IEEE Eng. Medicine Biology Soc. (EMBC), Milan, Italy, Aug. 2015, pp. 4820–4823.
25. M. Goršič et al., *Online phase detection using wearable sensors for walking with a robotic prosthesis*, Sensors **14** (2014), no. 2, 2776–2794.
26. A. Mannini and A. M. Sabatini, *Machine learning methods for classifying human physical activity from on-body accelerometers*, Sensors **10** (2010), no. 2, 1154–1175.
27. S. Mo and D. H. Chow, *Accuracy of three methods in gait event detection during overground running*, Gait Posture **59** (2018), 93–98.
28. I. Skog et al., *Zero-velocity detection—An algorithm evaluation*, IEEE Trans. Biomedical Eng. **57** (2010), no. 11, 2657–2666.
29. J. O. Nilsson, A. K. Gupta, and P. Händel, *Foot-mounted inertial navigation made easy*, in Proc. Int. Conf. Indoor Positioning Indoor Navigation (IPIN), Busan, Rep. of Korea, Oct. 2014, pp. 24–29.
30. Y. Blanc et al., *Temporal parameters and patterns of the foot roll over during walking: normative data for healthy adults*, Gait Posture **10** (1999), no. 2, 97–108.
31. T. Chau, *A review of analytical techniques for gait data. Part 2: neural network and wavelet methods*, Gait Posture **13** (2001), no. 2, 102–120.
32. S. Mallat, A wavelet tour of signal processing, Elsevier, 1999.
33. M. Antonini et al., *Image coding using wavelet transform*, IEEE Trans. Image Process. **1** (1992), 205–220.
34. P. S. Addison, J. Walker, and R. C. Guido, *Time–frequency analysis of biosignals*, IEEE Eng. Medicine Biology Mag. **28** (2009), no. 5, 14–29.
35. S. Khandelwal and N. Wickström, *Novel methodology for estimating Initial Contact events from accelerometers positioned at different body locations*, Gait Posture **59** (2018), 278–285.

AUTHOR BIOGRAPHIES

JeongKyun Kim received his MS degree in Computer Software from the University of Science and Technology, Daejeon, Rep. of Korea in 2017, and has been pursuing his PhD degree in ICT from University of Science and Technology since 2017. His research interests are in the broad areas of healthcare, signal processing, and machine learning.

Myung-Nam Bae received his MS and PhD degrees in Computer Science from Chonbuk National University, Chonju, Rep. of Korea, in 1993 and 1998, respectively. Since 1998, he has been with the Electronics and Telecommunications Research Institute, Daejeon, Rep of Korea. His current research interests include human body behavior analysis, intelligent IoT platforms, and response services for disaster situations.

Kang Bok Lee completed his PhD in Information and Communication Engineering from Chungbuk National University in 2002. He was a senior researcher at LG Semicon Co., Ltd. from 1993 to 2000. He has been a Principal researcher at ETRI since 2000. His research interests are in the areas of RFID/NFC, IoT services, and IoT sensor application technology.

Sang Gi Hong received his PhD degree in Electronic Engineering from Chungnam National University, Daejeon, Rep. of Korea in 2013. Since 2001, he has been with the Electronics and Telecommunications Research Institute, Daejeon, Rep. of Korea, where he has been working on IT convergence technologies. His current research interests include sensor signal processing, intelligent data processing, and IoT collaborative platform architecture for disaster management.